New results from a search for $\nu\_\mu \to \nu\_\tau$ and $\nu\_e \to \nu\_\tau$ oscillation

E. Eskut, A. Kayis-Topaksu, G. Onenguet, R. van Dantzig, M. de Jong, J. Konijn, O. Melzer, R G C. Oldeman, E. Pesen, C a F J. van der Poel, et al.

EUROPEAN ORGANIZATION FOR NUCLEAR RESEARCH

CERN-EP/2000-147
November 10, 2000

New results from a search for $\nu_\mu \rightarrow \nu_\tau$ and $\nu_e \rightarrow \nu_\tau$ oscillation

The CHORUS Collaboration

E. Eskut, A. Kayis-Topaksu, G. Onengüt
Çukurova University, Adana, Turkey

R. van Dantzig, M. de Jong, J. Konijn, O. Melzer, R.G.C. Oldeman, E. Pesen, C.A.F.J. van der Poel, J.W.E. Uiterwijk, J.L. Visschers
NIKHEF, Amsterdam, The Netherlands

M. Guler, M. Serin-Zeyrek, R. Sever, P. Tolun, M.T. Zeyrek
METU, Ankara, Turkey

N. Armenise, F. Cassol[1], M.G. Catanesi, M. De Serio, M.T. Muciaccia, E. Radicioni, P. Righini, S. Simone, L. Vivolo
Università di Bari and INFN, Bari, Italy

A. Bülte, K. Winter
Humboldt Universität, Berlin, Germany[2]

P. Annis[3], R. El-Aidi, M. Vander Donckt[4], B. Van de Vyver[5], P. Vilain[6], G. Wilquet[6]
Inter-University Institute for High Energies (ULB-VUB) Brussels, Belgium

B. Saitta
Università di Cagliari and INFN, Cagliari, Italy

E. Di Capua
Università di Ferrara and INFN, Ferrara, Italy

Y. Ishii[7], M. Kazuno, S. Ogawa, H. Shibuya
Toho University, Funabashi, Japan

J. Brunner[1], M. Chizhov[8], D. Cussans[9], M. Doucet[10], J.P. Fabre, W. Flegel, M. Litmaath[11], H. Meinhard, E. Niu[12], H. Øveràs, J. Panman, I.M. Papadopoulos, S. Ricciardi[13], A. Rozanov[1], D. Saltzberg[14], P. Strolin[15], R. Tsenov[8], C. Weinheimer[16], H. Wong[17], P. Zucchelli[18]
CERN, Geneva, Switzerland

J. Goldberg
Technion, Haifa, Israel

M. Chikawa
Kinki University, Higashiosaka, Japan

E. Arik, A.A. Mailov
Bogazici University, Istanbul, Turkey

J.S. Song, C.S. Yoon
Gyeongsang National University, Jinju, Korea

K. Kodama, N. Ushida
Aichi University of Education, Kariya, Japan

S. Aoki, T. Hara
Kobe University, Kobe, Japan

G. Brooijmans[4,11], D. Favart, G. Grégoire, J. Hérin[4]
Université Catholique de Louvain, Louvain-la-Neuve, Belgium

A. Artamonov[19], P. Gorbunov, V. Khovansky, V. Shamanov, I. Tsukerman
Institute for Theoretical and Experimental Physics, Moscow, Russian Federation

D. Bonekämper, N. D'Ambrosio, D. Frekers, D. Rondeshagen, T. Wolff[20]
Westfälische Wilhelms-Universität, Münster, Germany[2]

K. Hoshino, M. Komatsu, Y. Kotaka, T. Kozaki, M. Miyanishi, M. Nakamura, T. Nakano, K. Niu, K. Niwa, Y. Obayashi[21], O. Sato, T. Toshito[21]
Nagoya University, Nagoya, Japan

N. Bruski, S. Buontempo, A.G. Cocco, G. De Lellis[22], F. Di Capua, A. Ereditato, G. Fiorillo, T. Kawamura, R. Listone, M. Messina, P. Migliozzi, V. Palladino, V. Tioukov
Università Federico II and INFN, Naples, Italy

K. Nakamura, T. Okusawa
Osaka City University, Osaka, Japan

A. Capone, D. De Pedis, S. Di Liberto, U. Dore, P.F. Loverre, L. Ludovici, A. Maslennikov[23], G. Piredda, G. Rosa, R. Santacesaria, A. Satta, F.R. Spada
Università La Sapienza and INFN, Rome, Italy

E. Barbuto, C. Bozza, G. Grella, G. Romano, S. Sorrentino
Università di Salerno and INFN, Salerno, Italy

Y. Sato, I. Tezuka
Utsunomiya University, Utsunomiya, Japan

---

[1]Now at CPPM CNRS-IN2P3, Marseille, France.
[2]Supported by the German Bundesministerium für Bildung und Forschung under contract numbers 05 6BU11P and 05 7MS12P.
[3]Supported by Regione autonoma della Sardegna, Italy.
[4]Institut Interuniversitaire des Sciences Nucléaires.
[5]Nationaal Fonds voor Wetenschappelijk Onderzoek.
[6]Fonds National de la Recherche Scientifique.
[7]Deceased
[8]On leave of absence from St.Kliment Ohridski University of Sofia, Bulgaria.
[9]Now at University of Bristol, Bristol, UK.
[10]Now at DESY, Hamburg, Germany.
[11]Now at Fermi National Accelerator Laboratory, Batavia, IL, USA.
[12]Now at Center for Chronological Research, Nagoya University, Nagoya, Japan.
[13]Now at Royal Holloway College, University of London, Egham, UK.
[14]Now at U.C.L.A., Los Angeles, USA.
[15]On leave of absence from University of Naples "Federico II", Naples, Italy.
[16]Now at University of Mainz, Mainz, Germany.
[17]Now at Academia Sinica, Taipei, Taiwan.
[18] On leave of absence from INFN, Ferrara, Italy
[19]and CERN, Geneva, Switzerland
[20] Supported by a grant from Deutsche Forschungs Gemeinschaft.
[21]Now at Kamioka Observatory, Institute for Cosmic Ray Research, University of Tokyo, Gifu, Japan.
[22]Partially supported by the "Fondo Sociale Europeo".
[23]CASPUR, Rome, Italy.

Abstract

A first analysis of the complete set of data collected by CHORUS in the years 1994-1997 is presented. The search for ν_τ charged current events has been performed for both leptonic and hadronic decays of the τ lepton. No τ candidate has been found. A $\nu_\mu \rightarrow \nu_\tau$ mixing is excluded down to $sin^2 2\theta_{\mu\tau}$ = 6.8×10^{-4} for large $\Delta \mathrm{m}^2$ (90% C.L.).

To be published on Physics Letters B

1 Introduction

CHORUS is an experiment designed to search for $\nu_\mu \rightarrow \nu_\tau$ oscillation through the observation of charged current interactions ν_τ N $\rightarrow$ τ^- X, followed by the decay of the τ lepton. The search is sensitive to very small mixings if the mass difference is of the order of a few eV or larger. In a scheme where the mass difference is essentially coinciding with the ν_τ mass, the latter becomes a good candidate for the hot component of the Dark Matter of the Universe. This consideration constitutes the main motivation of the experiment.

The experiment was performed in the CERN Wide Band Neutrino Beam, which contains mainly ν_μ with a contamination of ν_τ well below the level of sensitivity that can be reached by this experiment. Neutrino interactions occur in a target of nuclear emulsions, whose spatial resolution (below one micrometer) allows a three dimensional *visual* reconstruction of the τ lepton and its decay products. The experiment is sensitive to most of the decay channels of the τ.

The Collaboration has already reported [1, 2] limits on $\nu_\mu \rightarrow \nu_\tau$ oscillation obtained from an analysis of a subsample of neutrino interactions. In this paper we describe in more detail the results of an analysis extended to the data sample collected in the four years of data taking (1994-1997). The present analysis is not the final one. In a second phase the sensitivity will be further improved.

2 The experimental setup

2.1 The neutrino beam

The West Area Neutrino Facility (WANF) of the CERN SPS provides an intense beam of ν_μ with an average energy of 27 GeV, well above the τ production threshold (E_ν= 3.5 GeV). The neutrino beam, besides the ν_μ component, also contains small fractions of $\overline{\nu}_\mu$, ν_e, $\overline{\nu}_e$. Fig.1 shows the spectrum of the various beam components, as resulting from a complete simulation of the beam, starting from the interaction of the primary protons. The $\overline{\nu}_\mu$, ν_e and $\overline{\nu}_e$ contents are 5.6%, 0.9% and 0.2% respectively. The figure also shows the tiny contamination of prompt ν_τ. Its contribution to the background to the oscillation search is discussed in section 8.

It is worth mentioning that the CHORUS detector is capable of a direct measurement of the spectral shapes and of the relative abundances of the two main components of the beam. In fact, the apparatus includes a large mass calorimeter followed by a muon spectrometer (described in detail in the next section). Besides neutrino interactions in the emulsion target, data were also collected using the calorimeter as a neutrino target. The calorimeter allows a high resolution measurement of hadronic showers. The spectrometer following the calorimeter provides the reconstruction of the muon and a precise measurement of its momentum. The analysis of the neutrino interactions in the calorimeter has allowed the cross-checking of various features of the MC simulation. In particular, agreement at the 10% level is found on the relative $\overline{\nu}_\mu/\nu_\mu$ fluxes [3].

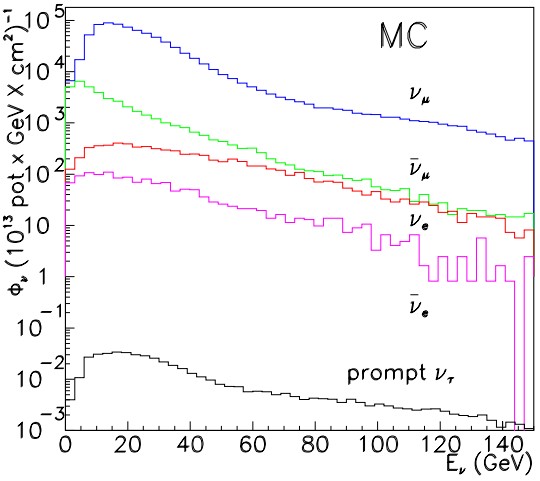

Figure 1: *Energy spectra of the various components of the neutrino beam (MonteCarlo simulation)*

2.2 The apparatus

A schematic picture of the CHORUS apparatus is shown in Fig.2.

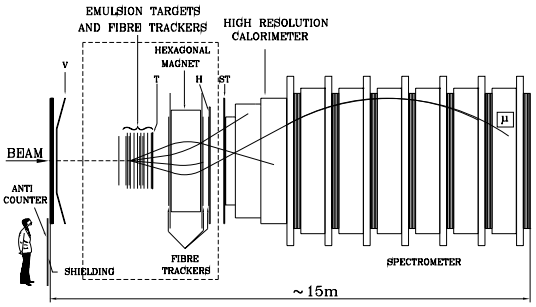

Figure 2: *General layout of the detector*

The *hybrid* setup, described in detail in Ref.[4], is composed of an emulsion target, a scintillating fiber tracker system, trigger hodoscopes, a magnetic spectrometer, a lead-scintillator calorimeter and a muon spectrometer.

The nuclear emulsions act as the target and, simultaneously, as detector of the interaction vertex and the decay point of the τ lepton [5]. The total mass of the target is 770 Kg. The emulsions are subdivided in 4 stacks of 36 plates, oriented perpendicularly to the beam and with a surface of 1.44×1.44 m^2. Each plate is made of a 90 μm transparent plastic film with 350 μm emulsion sheets on both sides. The nuclear emulsion target is equipped with a high resolution tracker made out of planes of emulsions and of planes of scintillating fibers. Each stack is followed by three special interface emulsion sheets: two Changeable Sheets (CS), close to

the fiber trackers, and a Special Sheet (SS), close to the emulsion stack. The sheets have a plastic base of 800 μm coated on both sides by 100 μm emulsion layers.

Eight planes of trackers of scintillating fibers (500 μm diameter) [6], interleaved between the emulsion stacks, reconstruct the trajectories of the charged particles with a precision of 150 μm in position and 2 mrad in angle at the surface of the CS. The layout of an emulsion stack is sketched in Fig.3.

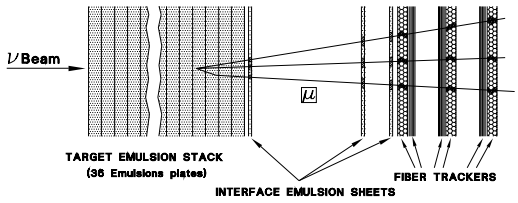

Figure 3: *Layout of an emulsion stack and associated fiber trackers*

Downstream of the target region, a magnetic spectrometer performs the reconstruction of charge and momentum of charged particles. An air-core magnet [7] of hexagonal shape produces a pulsed homogeneous field of 0.12 T. Field lines are parallel to the sides of the hexagon and the magnetised region extends for a depth of 75 cm in the direction of the beam. The tracking before and after the magnet is performed by a high resolution detector made of scintillating fibers (500 μm diameter) and complemented with few planes of electronic detectors (streamer tube chambers in the 1994, 1995 and the beginning of 1996 runs, honeycomb chambers [8] afterwards). The resulting momentum resolution $\Delta p/p$ is 30% at 5 GeV.

In addition to the detection elements described above, the air-core hexagonal magnet region has been equipped with emulsion trackers for the 1996 and 1997 runs. The aim was to perform a more precise kinematical analysis of the τ decay candidates.

A 100 ton *spaghetti* calorimeter (lead and scintillating fiber [9]) follows the magnetic spectrometer and measures the energy and direction of electromagnetic and hadronic showers.

The calorimeter is followed by a muon spectrometer made of magnetised iron disks interleaved with plastic scintillators and tracking devices. A momentum resolution of 19% is achieved by magnetic deflection for muons with momenta greater than 7 GeV. At lower momenta, the measurement of the range yields a 6% resolution.

3 Data collection

During the 4 years of operation the emulsion target has been exposed to the neutrino beam for an integrated intensity which corresponds to 5.06×10^{19} protons on target (pot). The data acquisition system recording the response of the electronic detectors was operational for 90% of the time. The average dead time for the emulsion interaction triggers was 12%. The trigger efficiency was 99% for charged current (CC) and 90% for neutral current (NC) events [10].

4 Principle of analysis

The search for ν_τ interactions has been performed for the following two decay modes of the τ lepton:

(1) $\tau^- \to \mu^- \nu_\tau \bar{\nu}_\mu$

(2) $\tau^- \to \mathrm{h}^-(n\pi^0)\nu_\tau$

Both decay modes give rise in the emulsions to a $kink$ topology: a track from the neutrino interaction vertex showing a change in direction after a short path (of the order of 1 mm at the energies typical for this experiment).

The information of the electronic detectors has been used to define two data sets, the 1μ and 0μ samples, distinguished by the presence or absence of one reconstructed muon of negative charge. For each sample few kinematical selections are applied to reduce the scanning load, while keeping a high sensitivity to the two decay modes of the τ. For the selected events, the track trajectories reconstructed in the fiber trackers are used to guide the scan in the pair of changeable sheets immediately following the stack containing the interaction vertex. The tracks are then followed in the special sheet and then in the target emulsion stacks where the search for the τ decay is performed. In the next two sections we give some detail on the selection of the two data sets, the 1μ and 0μ, and then we describe the scanning of the emulsions.

5 Data selection

The events kept for the analysis in the emulsions are those for which the scintillating fiber trackers allow track reconstruction and the determination of the interaction vertex position, with the reconstructed vertex position lying in the target emulsions. The event must contain at least one negative track, as a possible decay product of a τ. Note that events with only one reconstructed track were also kept, with the vertex position assumed to be in the middle of the emulsion stack immediately preceding the first plane of fiber tracker hit. The sample contains a few percent contamination of events with the reconstructed vertex wrongly assigned to the target emulsion, while the interaction actually took place in the surrounding material.

5.1 The 1μ events

An event belongs to the 1μ sample if it contains one reconstructed muon track of negative charge. The muon identification and reconstruction is based on the muon spectrometer response. Muons not reaching the spectrometer can in some cases be identified in the calorime-

ter. Momentum and charge are then measured, with lower precision, by the air-core magnet (for stopping muons the momentum is obtained from the range).

The efficiency for selecting CC events is about 80% and is the product of the efficiency for muon identification and that of the track and vertex reconstruction algorithms. Note that part of the inefficiencies are due to events where the muon track, though correctly identified in the muon spectrometer, does not match with the required precision the track reconstructed in the fiber trackers. Failures in the tracks and vertex reconstruction are mainly due to π^0's overlapping the tracks of charged secondaries.

The resulting 1μ sample consists of 713,000 events. The data set to be analysed for the search of τ decays was defined by the requirement that the event contains only one muon, with negative charge and momentum smaller than 30 GeV. The 30 GeV selection reduces by 29% the number of events to be scanned. The effect on possible ν_τ interactions depends on the oscillation parameters: the selection would reject 15% of the ν_τ interactions if the ν_τ had the same energy spectrum as the ν_μ. The actual loss in sensitivity is, however, much smaller, since a high energy muon implies most of the times a decay angle too small to be detected.

5.2 The 0μ events

The 0μ sample contains events where no muon is found. Events are selected if tracks have been reconstructed by the scintillating fiber trackers and the reconstructed vertex position lies in the target emulsions.

This sample consists of 335,000 events, with a calculated contamination of about 140,000 misidentified CC interactions and about 20,000 interactions generated by neutrinos other than ν_μ. Out of this sample we select for the emulsion analysis events with at least one track corresponding to a particle of negative charge and momentum in the 1 to 20 GeV interval. The lower bound reduces the large amount of low energy particles from secondary interactions or γ conversions. The upper bound is dictated by the poor momentum resolution at higher energy. A reliable momentum reconstruction has been obtained keeping only tracks which traverse the hexagonal air-core magnet without crossing any of its six spokes, so avoiding large multiple scattering. The momentum fit requires the presence of hits in all the tracking elements: the planes of fiber trackers and the chambers downstream of the air-core magnet (streamer tubes or honeycomb chambers, depending on the running periods). The number of tracks per event selected for the kink search may be larger than one.

5.3 The final samples

The negative track, hadron or muon, selected as a candidate for τ daughter has to satisfy further requirements. To allow the good functioning of the automatic scanning systems, the angle of the track with the beam axis has to be smaller than 0.4 rad. In view of the large background of muons originating from a nearby secondary beam, tracks at an angle smaller than 0.05 rad from the direction of this beam are also excluded (this selection was only applied on 1994 and 1995 data when the secondary beam was run at high intensity).

After all selections the 1μ and the 0μ data sets eligible for emulsion scanning consist of 477,600 and 122,400 events respectively. The events sent to the automatic scanning procedure – described in the next section – are fewer (355,395 and 85,211 respectively), mainly because of fiducial volume cuts imposed by the scanning technique and of the bad quality of a few emulsion plates.

The different stages of the reconstruction and selection procedure are summarised in Table 1.

The reconstruction inefficiencies, as well as those originating from the trigger, are well understood and reproduced by detailed MC simulations, both for the 1μ and the 0μ data sets.

6 Scanning procedure

6.1 Vertex location

The emulsion scanning procedure is fully automated using computer controlled microscopes equipped with CCD cameras and fast processors. The processor, which is called *track selector* [11], is capable of identifying tracks inside the emulsions, measuring their parameters on line.

The location of the plate containing the interaction vertex is based on the following back of the selected negative tracks, assumed to be the τ daughters. The track is first located in the interface emulsion sheets (CC and SS) with a search initially based on the track parameters measured by the scintillating fiber trackers. A track which is found in the interface emulsion sheets is followed upstream in the target emulsion stack, using track segments reconstructed in the most upstream 100 μm of each plate, until it disappears. The corresponding plate is defined as the vertex plate, since it should contain the primary neutrino vertex or the secondary (decay) vertex, or both, from which the track originates. The three most downstream plates of each stack are used to validate the matching with the interface emulsion sheets and are not considered as possible vertex plates. The efficiency of this scan-back procedure is almost independent from the track momentum and angle.

The number of located events is given in Table 1, separately for the 1μ and 0μ samples. For the 0μ sample a second number, given in brackets in the table, represents the events actually used for the decay search. This number is smaller than the number of located events because, after the reprocessing through an updated version of the reconstruction program, a fraction of the located events failed to pass the kinematical selections.

As confirmed by a detailed simulation of the scan-

Table 1: *Data flow chart*

Protons on target	5.06×10^{19}
1μ: events with 1 negative muon and vertex predicted in emulsion	713,000
1μ: $p_\mu < 30$ GeV and angular selections	477,600
1μ: events scanned	355,395
1μ: vertex located	143,742
1μ: events selected for eye-scan	11,398
0μ with vertex predicted in emulsion (CC contamination)	335,000 (140,000)
0μ with 1 negative track (p = 1-20 GeV and angular selections)	122,400
0μ: events scanned	85,211
0μ: vertex located (corrected number after reprocessing)	23,206 (20,081)
0μ: events selected for eye-scan	2,282

ning, there is a difference on the average location efficiency for 1μ (40%) and 0μ events (27%). The reconstruction of the muon in 1μ events is usually easier than that of the hadron in 0μ events because the latter is more often overlapping with other tracks from hadronic and e.m. showers. This leads in the first case to more reliable predictions of the track parameters, and hence to a higher location efficiency. Note that for the hadronic decay of the τ the vertex finding efficiency will be higher than that found for ν_μ NC interactions. In fact, coming from the decay of the τ, the followed track will generally be more isolated. The MonteCarlo simulation shows that in this case the vertex finding efficiency approaches the value found for the 1μ events.

6.2 Decay search

Once the vertex plate is defined, automatic microscope measurements are performed to select the events potentially containing a decay topology (kink). Different algorithms have been applied as a result of the progress in the scanning procedures and of the improving performance in speed of the scanning devices. The data can be subdivided in three sets according to the scanning methods:

- in the first procedure (applied to part of the 1994 data – mainly 1μ – and described in [1]) the event is selected either when a significant minimum distance between the scan-back track and any other predicted track is detected, or when the change in the scan-back track direction between the vertex plate and the exit from the emulsions corresponds to an apparent transverse momentum, p_T, larger than 250 MeV. For the selected events and for those with only one predicted track, digital images of the vertex plate are recorded and are analysed off-line for the presence of a kink. The number of located events treated with this method is about 18,000. The numbers of events selected for eye-scan by the automatic search are 5,768 for the 1μ and 276 for the 0μ sample.

- the second procedure is applied to all other events. It is restricted to the search of decay angles greater than 0.025 rad. In that case the vertex plate is assumed to contain the decay vertex of a charged parent produced in a more upstream plate. The upstream part of the vertex plate is scanned in order to find a track crossing within a small tolerance, the direction of the daughter candidate as sketched in Fig.4. This method also works for events where the decay vertex and the primary vertex occur in the same plate but on opposite sides of the plastic base. The method provides about 85% of the total kink finding efficiency. A total of 125,000 1μ events and all the 0μ events have been analysed with this method. Candidates for eye-scan from this search are 5,006 1μ and 1,823 0μ.

- a third search technique has been applied to 70% of the 1μ data of 1995, and to 75% of 1μ and 0μ data of 1996 and 1997. In this procedure, once the vertex plate is located by the scan-back track, a search is performed in that emulsion plate for all other tracks reconstructed by the fiber trackers. This scan allows a high precision comparison of the impact parameter of the scan-back track with respect to the vertex in emulsion defined by the other tracks. The method extends the sensitivity to smaller values of the decay path of the τ and contributes to about 15% of the total kink finding efficiency. Candidates for eye-scan from this search are 624 1μ and 183 0μ.

6.3 Eye-scan

A computer assisted eye-scan is performed for all the kink candidates selected during the automatic search. The aim of the eye-scan is to confirm the presence of a secondary vertex. An event is retained as a τ^- decay candidate if the secondary vertex appears as a kink without black prongs, nuclear recoils, blobs or Auger electrons. For the selected events the parent and decay particle, as well as the other tracks coming from the interaction vertex, are accurately measured. The measurements are used for the final topological and kinematical selections designed to reject the residual background. The efficiency of these procedures, the evaluation of the background, and the choice of the final selections are described in the next two sections.

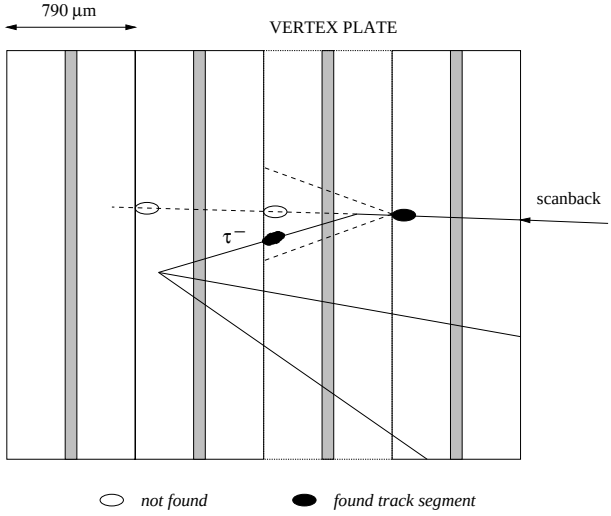

Figure 4: *Schematic view of the second decay search technique described in the text. The dotted lines indicate the cone around the scan-back track in which the search for the parent track is performed.*

7 Efficiency for the detection of ν_τ interactions

The efficiency for the detection of ν_τ interactions has been split into two terms: the first one, the acceptance A, is given by the efficiency of the reconstruction of the neutrino interaction by the electronic detectors and of the location in the emulsions. It also includes the few geometrical and kinematical selections applied before scanning. The second term, ϵ_{kink}, is the efficiency of the kink detection in the emulsions, multiplied by the efficiency of the geometrical and kinematical selections applied once the kink is found.

The error on the absolute value of the acceptance is mainly due to the uncertainties on the reconstruction and location efficiencies. However, these uncertainties affect in a similar way the acceptance for ν_τ and ν_μ induced events. Therefore, their effect largely cancels in the ratio of *observed* ν_τ to *observed* ν_μ events, used to compute the oscillation probability. More critical is the determination of ϵ_{kink}. For that parameter an experimental check of the calculated value is possible by using the data itself, as shown below.

The efficiencies for the signal and the background have been evaluated from large samples of events, generated according to the relevant processes, passed through a GEANT [12] based simulation of the detector response. The output was then processed through the same reconstruction chain used for the data. The response of the emulsion to charged particles was also simulated, so allowing the evaluation of the efficiencies of each step of the scanning.

A partial test of the kink finding efficiency has been carried out by studying hadron interactions. A small fraction of the scan-back tracks are in fact secondary particles originated by the interaction of a hadron in the emulsion, the hadron having been produced in turn in a neutrino interaction. The automatic scanning procedure detects the secondary interaction with an efficiency which is related in a simple way to the kink detection efficiency. As a by-product of part of the decay search applied to the 0μ sample, 80 neutrino events with a secondary hadron interaction have been detected. This result is in good agreement with the expected value of 84 computed with a MonteCarlo simulation. Although the decay and interaction topologies have some differences, the agreement constitutes a reliable check of the simulation of the automatic scanning procedure.

8 Background evaluation and final selections

The basic requirements adopted to isolate τ decay candidates are a selection, p_T larger than 250 MeV, on the transverse momentum of the decay particle with respect to the parent direction (to eliminate decays of strange particles), and a maximum length for the decay path. For the muonic decay of the τ, the kink must occur within five plates downstream of the neutrino interaction vertex plate. Because of the different background sources, a more severe and complicated selection on the decay pattern has been applied to the 0μ sample. This last selection will be examined after a discussion of all possible sources of background.

An unavoidable background to $\nu_\mu \rightarrow \nu_\tau$ oscillation is caused by the presence of prompt ν_τ's in the neutrino beam. Calculations [13] show that it is small compared to other sources of background. For the statistics considered in this paper it amounts to less than 0.1 events and has been neglected.

Apart from this, the background is constituted by any event having a negative track undergoing a deviation of its trajectory in the emulsion target. To obtain a realistic estimation of the number of events expected in absence of an oscillation signal, large samples of all the known background processes have been simulated and processed by the same reconstruction programs as the real data.

One source of background common to all the decay channels of the τ is due to charm production, namely:

- the production of negative charmed particles from CC interactions of the anti-neutrino components of the beam. These events constitute a background if the primary μ^+ or e^+ remains unidentified. Taking into account the appropriate cross-sections and the branching ratios, we expect in the present sample 0.11 events in the 1μ channel and 0.02 in the 0μ channel;
- the production of positive charmed mesons in CC interactions, if the primary lepton is not identified and the charge of the charmed particle daughter is incorrectly measured. In the present sample the expected background amounts to 0.7 events for the 0μ events. For the 1μ events the expected

Table 2: *Summary table of the expected background events. The observed number of events is also shown, together with the maximum number of ν_τ observable events (see text).*

		charm($\nu + \bar{\nu}$)	WK	Total	Observed	N_τ^{max}
1μ	$L_k < 5$ plates	0.1	-	0.1	0	5,014
0μ	$L_k < 3$ plates	0.7	2.6	3.3	4	2,791
	$(L_k(p_h))_{80\%}$	0.5	1.7	2.2	1	2,537
	$(L_k(p_h))_{80\%}$ and $\Phi_{(\tau-H)} > 90^o$	0.3	0.8	1.1	0	2,004

background amounts to less than 0.03 events and has been neglected. The fact that this background is much smaller in the 1μ sample is mainly due to the very low probability of a wrong measurement of the charge in the muon spectrometer;

- the associated charm production both in CC and NC interactions, when one of the charmed particles is not detected and, for CC events, the primary lepton is not identified. The cross-section for this reaction due to the NC interaction has been measured with large errors [14], while for the charged current process only an upper limit is available [14]. Within the present statistics the expected background amounts to less than 0.1 events in total and has been neglected in this analysis. Note that we are currently analysing data on charm production and a direct measurement of the cross-sections of associated charm production is being carried out.

For the decay into a single hadron the largest background rate is due to so-called hadronic *white kinks* (WK), defined as 1-prong nuclear interactions with no heavily ionising tracks or other evidence for nuclear break up (blobs or Auger electrons).

A robust estimation of this background comes from the study of WK events found during the τ kink search, at a distance between primary and secondary vertex outside the τ signal region. A total of 26 events with these characteristics were found over a total of 243 m of track length scanned back during the location procedure. Out of these, 8 events have an apparent decay p_T larger than 250 MeV. The corresponding effective WK interaction length is 24.0 ± 8.5 m. A similar result for the background expected before imposing the selection on p_T has been obtained by a preliminary analysis of the data collected by a dedicated experiment [15]. The experiment has performed WK measurements at CERN with the same emulsion as CHORUS, using pion beams of fixed momentum (2 to 5 GeV). That analysis also suggests that the background of events with p_T larger than 250 MeV is partly due to the limited momentum resolution and could therefore be reduced by improving the precision of the momentum measurement.

The ratio of WK events outside and inside the signal region has been determined with the help of a MonteCarlo simulation, based on FLUKA [16, 17]. The WK events expected within a distance, L_k, between the primary vertex and the kink point of three plates has been computed to be 2.6 ± 0.8.

This background can be further reduced by exploiting the difference of its kinematical properties with respect to those of the τ signal. Several selections on L_k have been considered: a simple cut at three plates, as in the past analyses, or selections dependent on the momentum of the scan back hadron, p_h. A better separation between signal and background is expected in the second case since the τ average decay length depends on the daughter momentum while a flat behaviour is predicted for WKs. A useful quantity to reject background events is the angle $\Phi_{(\tau-h)}$ in the plane transverse to the beam axis, between the direction of the parent candidate, measured in emulsion, and the hadronic shower axis. For true ν_τ events this angle is close to 180^o while, when the particle with the kink is part of the hadronic shower as in the WK or charm cases, the angular distribution is flatter, with more a preference for 0^o.

The optimisation of the selection has been done maximising the sensitivity to the oscillation, by computing the average limit that would be obtained with the given set of selections, by an ensemble of experiments with the same expected background and no expected signal. The most favorable choice turned out to be a selection on L_k retaining a fixed fraction of 80% of the τ signal in all p_h bins and the condition $\Phi_{(\tau-h)} > 90^o$. In Table 2 a summary of the results of the background computation is reported. The table gives the calculated number of background events and the number of observed events with various kinematical selections. In all cases, the number of observed events is consistent with the expected background. This shows, together with the reliability of the backgrond calculation, the lack of any evidence of ν_τ interactions. The chosen set of selections corresponds to zero observed events.

The maximum of the sensitivity is obtained through a compromise between low background and high efficiency for ν_τ detection. To illustrate that efficiency, the last column of Table 2 also displays N_τ^{max}, the number of ν_τ events which would be observed in case all incident ν_μ had converted into ν_τ. For the 1μ sample this number is given by:

$$(N_\tau^{max})_{1\mu} = N_{1\mu}^{loc} \cdot r_\sigma \cdot r_A \cdot \epsilon_{kink} \cdot Br_\mu \qquad (1)$$

where:

Table 3: *Efficiency for the decay detection and relative acceptance, for the τ decay modes contributing to the 0μ sample*

decay mode	Br	ϵ_{kink}	r_A	Br $\times\epsilon_{kink} \times r_A$
$\tau \to \nu_\tau h^- n h^0$	0.495	0.11	2.88	0.157
$\tau \to \nu_\tau \bar{\nu}_e e^-$	0.178	0.05	2.21	0.020
$\tau \to \nu_\tau \bar{\nu}_\mu \mu^-$	0.174	0.10	0.69	0.012

- $N_{1\mu}^{loc}$ is the number of located 1μ events ($N_{1\mu}^{loc} = 143,742$) ;
- $r_\sigma =< \sigma_\tau^{CC} > / < \sigma_\mu^{CC} >$ is the neutrino energy weighted CC cross-section ratio. A value $r_\sigma = 0.53$ has been used; it takes into account quasi-elastic interactions, resonance production and deep inelastic reactions;
- $r_A =< A_\tau > / < A_\mu >$ is the cross-section weighted acceptance ratio for ν_τ and ν_μ interactions. A_τ and A_μ take into account the effect of geometrical and kinematical selections applied before scanning and the reconstruction and location efficiencies. The values of r_A is close to one (r_A = 0.97);
- ϵ_{kink} includes the efficiency of the decay search procedure and that of the geometrical and kinematical selections applied after the kink is found. Its average value is 0.39;
- $Br_\mu = 17.4\%$ is the branching ratio of the decay $\tau \to \nu_\tau \bar{\nu}_\mu \mu^-$.

The formula giving N_τ^{max} for the 0μ sample is more complicated because of the contribution of different decay modes of the τ. The expression is:

$$(N_\tau^{max})_{0\mu} = N_{0\mu}^{loc} \cdot r_\sigma \cdot \sum_{i=1,3} r_{A_i} \cdot \epsilon_{kink_i} \cdot Br_i \quad (2)$$

where $N_{0\mu}^{loc}$ is the number of located 0μ events (20,081) and r_σ is the same cross-section ratio appearing in eq. 1. The three decay modes which contribute to the 0μ category are the τ decay in a negative hadron plus neutrals: $\tau \to \nu_\tau h^- n h^0$; the decay $\tau \to \nu_\tau \bar{\nu}_e e^-$, when the electron behaves similarly to a hadron (no early showering); the decay $\tau \to \nu_\tau \bar{\nu}_\mu \mu^-$, for the fraction of events where the muon is not identified but is still selected by the 0μ criteria. Table 3 displays the branching ratios of these three channels together with the values of ϵ_{kink}, computed for the final selection as defined in the last line of Table 2, and of r_A. The interpretation of the values of r_A, the ratio of acceptances, is in this case not straightforward. In fact, the acceptance for ν_μ interactions takes into account the NC/CC cross-section ratio, since the main contribution to the $N_{0\mu}^{loc}$ sample comes from NC interactions (note that in eq. 2, r_σ is the ratio of CC cross-sections). The kinematical selections have largely different effects on ν_μ and ν_τ interactions and also the reconstruction efficiency, which is included in the acceptance, is in this case different for ν_μ and ν_τ, as explained at the end of section 6.1.

In concluding this section, we recollect the final result of the search as displayed in Table 2. No τ decay candidate is found, neither in the 1μ sample nor in the 0μ sample, once the best set of selections is applied (last line of Table 2). The null observation is used to set limits on oscillation parameters. This is shown in the next section.

9 Limits on oscillation

Limits on $\nu_\mu \to \nu_\tau$ and $\nu_e \to \nu_\tau$ oscillation have been computed on the basis of zero candidates as observed both in the 1μ and 0μ samples.

9.1 Limits on $\nu_\mu \to \nu_\tau$ oscillation

Within a two flavours mixing scheme, the oscillation probability is written in the usual form:

$$P_{\mu\tau} = sin^2 2\theta_{\mu\tau} \cdot sin^2 \left(\frac{1.27 \cdot \Delta m^2 \cdot L}{E} \right) \quad (3)$$

The average values of L and E_{ν_μ} are 0.6 Km and 27 GeV respectively.

For large Δm^2 values, when the energy dependent term of the probability averages to 1/2, the upper limit on the oscillation probability is obtained from the equation:

$$P_{\mu\tau} \leq \frac{N_\tau}{(N_\tau^{max})_{1\mu} + (N_\tau^{max})_{0\mu}} \quad (4)$$

where, in the absence of a signal, N_τ is the upper limit on the number of τ decay candidates (the derivation of the upper limit will be discussed later in the text) and the two N_τ^{max} are defined in the previous section. When Δm^2 is comparable or smaller than the E/L ratio the spectrum of the ν_τ resulting from oscillation is modified by the energy dependent term of eq. 3. Then, to compute limits on the oscillation parameters, appropriate integrations are performed to take into account the effect of energy dependent cross-sections, acceptances and efficiencies. Fig.5 shows the dependence from the neutrino energy of the global analysis efficiency, $A_\tau \cdot \epsilon_{kink}$, of ν_τ interactions. It includes the effects of the full analysis chain i.e. the event reconstruction, the vertex location, the kink search and the kinematical cuts.

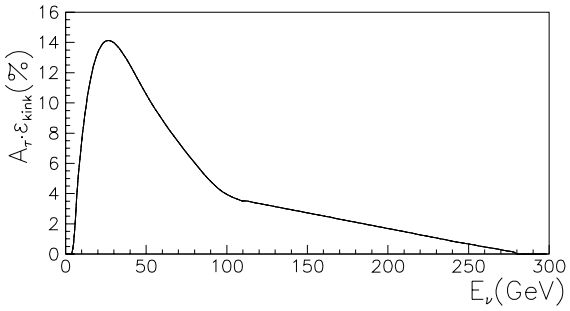

Figure 5: *Total efficiency, $A_\tau \cdot \epsilon_{kink}$, for ν_τ interactions detection as a function of the neutrino energy.*

The decrease at high energy is mainly due to the cuts applied on the momentum of the τ daughter candidate before scanning.

The size of the upper limit N_τ is determined by the statistics and by the systematic error affecting the denominator of eq. 4. The latter receives different contributions. The errors on the τ branching ratios and from the MonteCarlo statistics are negligible. The error on the $\sigma_\tau^{CC}/\sigma_\mu^{CC}$ ratio is also small. The calculation of the acceptances and an experimental check of the kink detection efficiency were discussed in section 7. We estimate the overall systematic error on the denominator of eq. 4 to be 17%.

For the determination of N_τ, i.e. the upper limit on the number of ν_τ candidates, we have used the method proposed by Junk [18] which allows the combination of different channels, taking into account the errors on the background and on the signal.

The overall 90% C.L. upper limit on the number of τ decays is 2.4. It is based on the null observation in the two independent channels, 1μ and 0μ. The limit on the $\nu_\mu \rightarrow \nu_\tau$ oscillation probability obtained through eq. 4 is:

$$P_{\mu\tau} \leq 3.4 \times 10^{-4} \qquad (5)$$

The 90% C.L. excluded region in the ($sin^2 2\theta_{\mu\tau}$, Δm^2) parameter space is represented in Fig.6. Full mixing between ν_μ and ν_τ is excluded at 90% C.L. for $\Delta m^2 > 0.6\ eV^2$. Large Δm^2 values are excluded at 90% C.L. for $sin^2 2\theta_{\mu\tau} > 6.8 \times 10^{-4}$.

Fig.6 also displays the recent NOMAD result [23]. Their result should not be directly compared with ours, since the statistical treatment of the data is different. The problem of calculating upper limits has recently received great attention. Many different methods have been suggested, consistently with the fact that different, statistically correct choices can be made to evaluate 90% C.L.. The NOMAD Collaboration has adopted the technique proposed by Feldman and Cousins (FC) [24] which, applied to our data – zero events observed – gives an upper limit of 1.4 events, much more stringent than

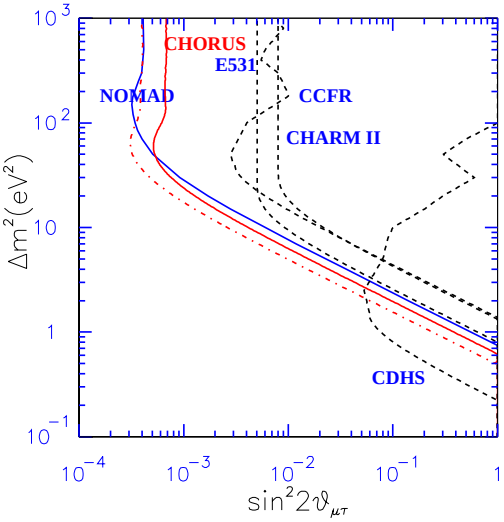

Figure 6: *Present limit on $\nu_\mu \rightarrow \nu_\tau$ oscillation compared to the results of previous experiments [19, 20, 21, 22] (dashed lines) and to the the recent NOMAD result [23] (full line); the meaning of the second CHORUS curve (dash–dotted), is explained in the text.*

the one we have used to draw the exclusion curve. The tightness of the upper limit resulting from the FC method in some particular cases, has already been questioned in the literature [25, 26]. We agree with the observation by Cousins [27] that these results are understood and statistically correct, since they reflect the low probability of the observed data set for a given expectation of background plus signal. However, the upper limit of 2.4 events, equally well founded statistically, gives information more directly connected to the common use of an exclusion plot, since it is related to the size of that signal which would have less than 10% probability of resulting in the observation of zero events. Note that results close to 2.4 are obtained using techniques other than the one proposed by Junk (see e.g. [25, 26]).

For the sake of a direct comparison with the result of NOMAD, the curve corresponding to the upper limit of 1.4 events ($sin^2 2\theta_{\mu\tau} < 4.0 \times 10^{-4}$ for large Δm^2) is also shown in Fig.6 (dash–dotted line).

9.2 Limits on $\nu_e \rightarrow \nu_\tau$ oscillation

The SPS neutrino beam contains a ν_e component which amounts to 0.9% of the integrated ν_μ flux. The negative result of the search for ν_τ interactions can therefore be used to set limits on the $\nu_e \rightarrow \nu_\tau$ oscillation. The evaluation of the limit has been performed with the same technique used for the $\nu_\mu \rightarrow \nu_\tau$ oscillation, this time in the assumption that the N_τ events are coming from the oscillation of the ν_e component of the beam. To account for the uncertainty on the ν_e/ν_μ flux ratio

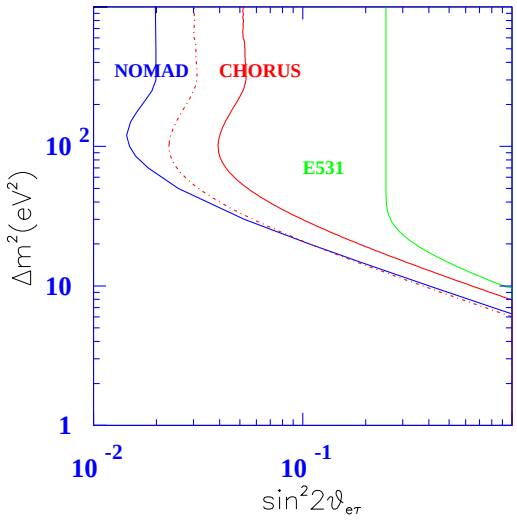

Figure 7: *Present limit on $\nu_e \rightarrow \nu_\tau$ oscillation compared to the result of E531 [19] and to the recent NOMAD result [23]; the meaning of the second CHORUS curve (dash–dotted), is explained in the text.*

the overall systematic error has been increased to 28% in this case. The difference between the ν_μ and ν_e energy spectra - the average energy of ν_e component is 13 GeV higher - leads to differences in the acceptance for ν_τ interactions. In the case of the ν_e beam, the increase of the cross-section with energy improves the sensitivity to ν_τ interactions, while the kinematic constraints and reconstruction inefficiencies affecting high energy events contribute to lower the acceptance.

Using the present sample the following 90% C.L. limit has been obtained

$$P_{e\tau} \leq 2.6 \times 10^{-2} \qquad (6)$$

The 90% C.L. excluded region in the ($sin^2 2\theta_{e\tau}$, Δm^2) parameter space is shown in Fig.7, together with the recent NOMAD [23] result. Full mixing between ν_e and ν_τ is excluded at 90% C.L. for $\Delta m^2 > 7.5\ eV^2$; large Δm^2 values are excluded at 90% C.L. for $sin^2 2\theta_{e\tau} > 5.2 \times 10^{-2}$.

The dash–dotted curve represents the result obtained by applying to our data the statistical method adopted by NOMAD.

10 Conclusions

The data collected by CHORUS in its four years of activity (1994-1997) have been analysed searching for the 1-prong decay of the τ. No evidence for ν_τ interactions has been found and stringent limits on the parameters of the oscillation have been set.

In the future the sensitivity of the experiment will be extended to reach its design value ($P_{\mu\tau} = 1 \times 10^{-4}$). Primary factors to achieve this goal are the substantial progress in the automatic scanning speed and various improvements in the reconstruction programs. It is now possible to scan more tracks per event and to digitize the emulsion grains in the vertex region for all located events. This will allow to increase the vertex location efficiency and to perform a detailed analysis of the located events, with a consequent increase of the kink detection efficiency as well. Work for an improvement in the hadron momentum measurement is in progress. It should allow to reduce the expected WK background.

Acknowledgements

We gratefully acknowledge the help and support of our numerous technical collaborators who contributed to the detector construction, operation, emulsion pouring, development and scanning. We thank the neutrino beam staff for their competent assistance in ensuring the excellent performance of the facility. The accumulation of a large data sample in this experiment has been made possible also thanks to the efforts of the crew operating the CERN PS and SPS. The general technical support from CERN EP(PPE, ECP) and IT(CN) divisions is warmly acknowledged.

The experiment has been made possible by grants from: the Institut Interuniversitaire des Sciences Nucléaires and the Interuniversitair Instituut voor Kernwetenschappen (Belgium), the Israel Science foundation (grant 328/94) and the Technion Vice President Fund for the Promotion of Research (Israel), CERN (Geneva, Switzerland), the German Bundesministerium für Bildung und Forschung (Germany), the Institute of Theoretical and Experimental Physics (Moscow, Russia), the Istituto Nazionale di Fisica Nucleare (Italy), the Promotion and Mutual Aid Corporation for Private Schools of Japan and Japan Society for the Promotion of Science (Japan), the Korea Research Foundation Grant (KRF - 99 - 005 - D00004) (Republic of Korea), the Foundation for Fundamental Research on Matter FOM and the National Scientific Research Organization NWO (The Netherlands) and the Scientific and Technical Research Council of Turkey (Turkey). We gratefully acknowledge their support.

Two of the authors, A.Arik and A.A.Mailov, wish to acknowledge their collaboration with S.Sultansoy.

References

[1] E. Eskut *et al.*, CHORUS Collaboration, Phys. Lett. **B424** (1998) 202.

[2] E. Eskut *et al.*, CHORUS Collaboration, Phys. Lett. **B434** (1998) 205.

[3] R.G.C. Oldeman, PhD Thesis, University of Amsterdam, June 2000.

[4] E. Eskut *et al.*, CHORUS Collaboration, Nucl. Instr. and Meth. **A401** 7 (1997).

[5] S. Aoki *et al.*, Nucl. Instr. and Meth. **A447** 361 (2000).

[6] P. Annis *et al.*, Nucl. Instr. and Meth. **A412** 19 (1998).
[7] F. Bergsma *et al.*, Nucl. Instr. and Meth. **A357** 243 (1995).
[8] J.W.E. Uiterwijk *et al.*, Nucl. Instr. and Meth. **A409** 682 (1998).
[9] E. Di Capua *et al.*, Nucl. Instr. and Meth. **A378** 221 (1996).
[10] M.G. van Beuzekom et al., Nucl. Instr. and Meth. **A427** 587 (1999).
[11] S.Aoki et al., Nucl. Instr. and Meth. **B51** 446 (1990).
[12] GEANT 3.21, CERN Program Library Long Writeup W5013.
[13] B. Van der Vyver, Nucl. Instr. and Meth. **A385** 91 (1997).
[14] N. Ushida *et al.*, E531 Collaboration, Phys. Lett. **B206** 375 (1988).
[15] A. Bülte *et al.*, CHARON experiment, http://www.cern.ch/charon.
[16] A. Fassò, A. Ferrari, J. Ranft and P.R. Sala, SARE-3 Workshop, KEK-Tsukuba, KEK Report Proceedings 97-5, p. 32 (1997).
[17] A. Ferrari, T. Rancati and P.R. Sala, SARE-3 Workshop, KEK-Tsukuba, KEK Report Proceedings 97-5, p. 165 (1997).
[18] T. Junk, Nucl. Instr. and Meth. **A434** 435 (1999).
[19] N. Ushida *et al.*, Phys. Rev. Lett. **57** (1986) 2897.
[20] F. Dydak *et al.*, CDHS Collaboration, Phys. Lett. **B134** (1984) 103.
[21] M. Gruwé *et al.*, CHARMII Collaboration, Phys. Lett. **B309** (1993) 463.
[22] K.S. McFarland *et al.*, CCFR Collaboration, Phys. Rev. Lett. **75** (1995) 3993.
[23] J. Astier *et al.*, NOMAD Collaboration, Phys. Lett. **B483** (2000) 387
[24] G.J. Feldman, R.D. Cousins, Phys. Rev. **D57** 3873 (1998).
[25] B.P. Roe, M.B.Woodroofe, Phys. Rev. **D60** 053009 (1999).
[26] G. Punzi, hep-ex/9912048
[27] R.D. Cousins, talk at the Workshop on Confidence Limits, CERN, 17-18 January 2000, http://cern.web.cern.ch/CERN/Divisions/EP/Events/CLW/papers.html